

Efficacy of Artificial Neural Network and Adaptive Neuro-Fuzzy Inference System Models in Scour Depth Prediction at Submerged Weirs

Javed Alam, Md Atif Raza, and Mohd. Muzzammil (2025)

Zakir Hussain College of Engineering and Technology, Aligarh Muslim University, Aligarh (Uttar Pradesh), INDIA

DOI: <https://doi.org/10.14796/JWMM.C553>

ABSTRACT

Accurate assessment of scour depth is crucial for the safe design of hydraulic structures, particularly around submerged weirs, where the scouring process is inherently complex due to intricate sediment transport and scour mechanisms. Although several studies have addressed scour at submerged weirs, the literature reveals limited investigations. Traditionally, scour depth prediction models have relied on regression analysis of laboratory data. However, recent advancements in soft computing techniques have shown superior predictive capabilities for complex modeling problems. This study uses soft computing models, specifically Artificial Neural Networks (ANN) and Adaptive Neuro-Fuzzy Inference Systems (ANFIS), to predict scour depth at submerged weirs. These models are trained and validated using existing experimental data from the literature. Our analysis demonstrates that ANN and ANFIS outperform conventional regression models in predicting scour depth. The conventional Feed-Forward Backpropagation (FFBP) neural network yielded the highest predictive accuracy among the soft computing approaches. Additionally, sensitivity analysis identified flow intensity and relative weir height as the most influential parameters affecting relative scour depth. These findings underscore the potential of soft computing techniques in enhancing the reliability of scour depth predictions for hydraulic design applications.

1. INTRODUCTION

Weirs are low-head hydraulic structures constructed across streams to achieve several critical functions: elevating upstream water levels, reducing flow velocities, river training, diverting flows, protecting banks, maintaining navigable water depths, and controlling channel bed degradation. These versatile structures are integral to the management and stabilization of waterways. Weirs can be classified based on their interaction with downstream water levels. When the tailwater depth on the downstream side is less than the weir height, the structure is termed an unsubmerged weir under free-flow conditions. In this scenario, scouring downstream

Alam, J., M.A. Raza, and M. Muzzammil. 2025. "Efficacy of Artificial Neural Network and Adaptive Neuro-Fuzzy Inference System Models in Scour Depth Prediction at Submerged Weirs." *Journal of Water Management Modeling* 33: C553. <https://doi.org/10.14796/JWMM.C553> www.chijournal.org ISSN: 2292-606 © Alam et al. 2025

of the weir is primarily driven by the direct impact of the jet stream on the sediment bed. Conversely, when the tailwater depth exceeds the weir height, the structure is known as a submerged weir under submerged flow conditions. For submerged weirs, the local scour process is more complex and is influenced by factors such as the intensity of the approaching flow and the flow regime over the weir. In sloping channels, a series of submerged weirs is often constructed to mitigate channel bed degradation and promote bed stabilization. These consecutive weirs effectively segment the channel bed into several partitions, reducing the longitudinal slope towards an equilibrium state and limiting further degradation. This partitioning strategy is crucial in preserving the structural integrity of the channel and maintaining its functionality over time.

Recently, experimental studies have focused extensively on the local scouring process around rectangular weirs under submerged flow conditions. These investigations aim to understand better the complex interactions between the flow and the sediment bed in the vicinity of submerged weirs, which are critical for the stability and design of hydraulic structures. Guan et al. (2013) conducted an in-depth analysis of the impact of bed load on scouring around submerged weirs. Their research revealed that under live bed scour conditions—where sediment transport is actively occurring—the scour depth downstream of the weir reaches its peak swiftly. This maximum scour depth is achieved relatively quickly due to the dynamic interaction between the flowing water and the movable sediment bed. Furthermore, Guan et al. (2013) observed that after reaching this peak, the downstream scour depth fluctuates around an average value. These fluctuations are attributed to the formation and migration of bed forms, such as dunes and ripples, which continuously alter the local flow patterns and sediment distribution. The bed forms dynamically interact with the flow, causing periodic changes in the scouring process and thus leading to the observed fluctuations in scour depth.

The insights gained from these studies are crucial for predicting the behaviour of submerged weirs in natural and engineered waterways. Understanding how factors like bed load and flow conditions influence scour can inform the design and placement of these structures to mitigate potential erosion and maintain their functional integrity over time. Guan et al. (2014a) conducted a comprehensive experimental investigation into the intricate flow dynamics, turbulence structures, and shear stress distributions within the downstream scour hole at submerged weirs under clear water scour conditions. They found that high-velocity jets and complex vortices play crucial roles in sediment entrainment and the development of the scour hole. Shear stresses are highest near the base of the weir, driving initial scouring and decreasing downstream, influencing sediment deposition. Their study provides valuable insights into the complex interactions between flowing water and the erodible bed material contributing to scour formation and evolution.

Guan et al. (2014b) investigated the effects of live bed scour on submerged weirs. They observed that the maximum scour depth upstream of the weir is strongly influenced by the steepness of approaching bedforms and inversely related to weir height. Additionally, they noted that the flow regime transitions from a surface jet to an impinging jet as the water level difference across the weir increases, each associated with distinct scour mechanisms downstream. Guan et al. (2015) examined the scour processes under live-bed conditions, where sediment transport significantly affects the scour formation upstream and downstream of the weir. They found that the scour depths and patterns are highly dynamic and influenced by the approach flow velocity and sediment supply. They identified that the equilibrium scour depth is

closely linked to the flow regimes over the weir and proposed a classification system for these regimes. This classification includes surface flow regime (SFR), transition regime (TR), and impinging jet regime (IJR), each associated with distinct scour profiles.

Bormann and Julien (1991), Gaudio et al. (2000), and Lenzi et al. (2003) provided early predictions of downstream scour depths under free-fall jet conditions. However, as Guan et al. (2015) noted, these models often did not account for the complexities introduced by submerged conditions, particularly under live-bed scenarios where bedforms and suspended loads play critical roles. They proposed a scour depth prediction model for different flow regimes over the weir. Guan et al. (2016) extended the previous research by investigating the effects of sediment size and tailwater depth on local scour at submerged weirs in sand-bed channels. Their study demonstrated that while the general flow regimes over the weir are unaffected by sediment size, the equilibrium scour depth is influenced by the sediment characteristics and the tailwater depth. They proposed new empirical equations that incorporate these factors to predict the equilibrium scour depths upstream and downstream of submerged weirs. Submerged weirs with sloped upstream faces are common in engineering design, yet there is limited understanding of how these slopes influence scour patterns. Wang et al. (2018a) addressed this research gap by investigating the impact of upstream weir slopes on local scour through a series of experiments. The study involved 62 tests conducted in a tilting recirculating flume using coarse and fine sands. Four different weir slopes were tested for each sand type to assess the variations in scour depth. The study found that the upstream slope did not affect the upstream scour depth for clear water scour conditions, and the downstream scour depth was independent of the upstream slope.

For live-bed scour conditions, a flatter upstream slope reduced the scour depth for both sands. A critical slope angle was identified, beyond which the effects of the slope on scour depth were minimized. Wang et al. (2018a) proposed new predictors for average scour depth that include the effects of upstream weir slope. Wang et al. (2018b) conducted a comprehensive experimental study to understand the effects of different downstream weir slopes on local scour using both coarse and fine sands. They found that the depth of scour upstream of the weir is independent of the downstream weir slope. When the downstream weir slope is greater than the upstream slope of the downstream scour hole, the downstream weir slope does not affect the downstream scour depth. However, when the downstream weir slope is less than the upstream slope, part of the downstream weir surface is exposed to the flow, increasing the downstream scour depth. The interaction between the weir slope and the flow can cause deflection of the overflow jet, influencing scour patterns. Specifically, a steep downstream slope can align the jet with the weir surface, exacerbating scour.

The study by Wang et al. (2018b) also proposed a conservative design method to account for the observed effects of downstream weir slopes on local scour. This method aims to enhance the safety and effectiveness of submerged weir designs by considering the rising upstream water level and the deflection of the overflow jet. Wang et al. (2019) experimentally examined the effect of weir height, flow intensity, and sediment coarseness on local scour at the submerged weir. They provided a comprehensive evaluation of existing scour depth predictors and highlighted the limitations of traditional models when applied to submerged conditions. They integrated new experimental data to enhance the accuracy of scour depth predictions, particularly for fully submerged weirs. Wang et al. (2020) further advanced the field by investigating the temporal evolution of clear water scour depth at submerged weirs. They

introduced a normalized time to reach equilibrium scour depth (t_e^*), which depends on flow intensity, sediment size, and weir dimensions. This scale helps predict the time required for scour to reach equilibrium, offering a more nuanced understanding of scour processes over time. Wen et al. (2021) investigated the flow field characteristics within developing scour holes using particle tracking velocimetry (PTV). They observed that the submerged weir significantly alters the mean flow, creating a high-velocity zone above the weir and complex vortex systems near the scoured bed. As the scour progresses, zones of high turbulence intensity and near-bed Reynolds shear stress shift closer to the upstream slope, affecting the sediment dynamics and stability of the scour hole.

Guan et al. (2022) extended the understanding of these processes by examining the fluctuating frequencies of scour depths around submerged weirs at equilibrium stages. They found that the upstream scour depth fluctuates at a frequency like the approaching bed forms, while downstream scour depth fluctuations occur at 0.38 to 0.68 times the frequency of the bedforms. This discrepancy is attributed to the different sediment transport mechanisms and flow dynamics on either side of the weir. Upstream, the sediment transport is dominated by bed load movement over the weir crest, whereas downstream, the deeper flow leads to more significant bedform development and slower sediment transport. The work by the stated researchers highlights the complex interactions between flow, sediment transport, and scour processes, providing valuable insights into designing and managing river training structures to mitigate adverse effects and enhance stability.

The above-mentioned studies on local scour around submerged weirs primarily focused on experiments conducted with uniform sediment beds. While these studies have significantly advanced the understanding of scour mechanisms. Their prediction models were based on the traditional regression method. Recent advancements in soft computing techniques have shown promise in modeling complex hydraulic phenomena to address the limitations of traditional empirical and regression-based models. These techniques include Artificial Neural Networks (ANN), Gene Expression Programming (GEP), Group Method of Data Handling (GMDH), and Adaptive Neuro-Fuzzy Inference System (ANFIS). Each method offers unique strengths in handling non-linear relationships and interactions within the data, making them well-suited for predicting hydraulic behaviour, such as scour depth under diverse conditions. In recent years, various soft computing techniques have been employed to model and predict the dimensions of scour holes around hydraulic structures. These methods have shown considerable promise in improving the accuracy of predictions over traditional empirical approaches.

Azamathullah et al. (2005) investigated the performance of three neural network models—Feed Forward Back Propagation (FFBP), Feed Forward Cascade Correlation (FFCC), and Radial Basis Function (RBF)—for predicting scour hole dimensions at ski-jump bucket spillways. They concluded that the FFBP model provided superior predictions compared to the FFCC and RBF models. Soliman (2007) applied the FFBP neural network to model the scour hole dimensions in stilling basins, finding that the FFBP model offered more promising results than traditional methods. Similarly, Noori and Hooshyaripor (2014) used the FFBP model to predict the scour hole dimensions downstream of ski-jump bucket spillways, demonstrating that FFBP outperformed empirical formulas. Roushangar et al. (2016) compared the modeling capabilities of FFBP and GEP for predicting downstream scour depth at various structures, including inclined slope grade control structures, sharp-crested weirs, and ski-jump buckets. They found that both FFBP and GEP provided better prediction performance than conventional regression models.

Azamathullah et al. (2009) evaluated the performance of ANFIS in estimating scour location downstream of bucket spillways, finding it highly satisfactory compared to regression models. Farhoudi et al. (2010) applied ANFIS to model the maximum scour depth, pattern, and time evolution of scour holes in United States Bureau of Reclamation (U.S.B.R.) type I stilling basins, reporting better results than those obtained from regression models. Keshavarzi et al. (2012) compared ANN and ANFIS for simulating scour around arch-shaped bed sills, concluding that ANFIS provided better predictive performance than ANN. Muzzammil and Alam (2016) modeled downstream scour depth at grade control structures using ANFIS and FFBP neural networks, with ANFIS proving to be superior to the FFBP model. The collective findings from these studies indicate that advanced soft computing techniques such as FFBP and ANFIS offer significant improvements over traditional regression models for predicting scour dimensions around various hydraulic structures. They also emerge as the most robust and accurate, capable of handling the complexities and non-linearities inherent in scour processes. The present study has comprehensively analyzed existing literature data on scour around submerged weirs. This analysis integrates data from multiple sources. The aim is to consider all relevant parameters examined by these authors to develop a robust prediction model for scour depth using regression analysis. In addition to traditional regression methods, this study also explores the potential of advanced soft computing techniques. Artificial Neural Networks (ANN) and Adaptive Neuro-Fuzzy Inference System (ANFIS) are employed to develop alternative prediction models for scour depth. These techniques are well regarded for their ability to handle non-linear and complex relationships in data, making them suitable for modeling hydraulic phenomena.

2. SCOUR PARAMETERS AND DIMENSIONAL ANALYSIS

The scour at submerged weir and related parameters are shown in Figure 1. The equilibrium downstream scour depth ($d_{s,a}$) at a submerged weir can be expressed as a function of several key parameters as given in Equation 1.

$$d_{s,a} = f(\rho, \rho_s, \mu, g, h_0, h_t, U_0, U_c, d_{50}, z, \alpha) \quad (1)$$

Where:

- ρ = fluid density,
- ρ_s = sediment density,
- μ = fluid viscosity,
- g = gravitational acceleration,
- h_0 = approach flow depth,
- h_t = tailwater depth,
- U_0 = average approach flow velocity,
- U_c = critical velocity of the approach flow,
- d_{50} = mean diameter of bed particles,
- z = weir height, and
- α = upstream weir face angle.

In particular, the approach flow depth (h_0) is influenced by the average approach flow velocity (U_0) and weir height (z), assuming a constant tailwater depth (h_t) (Guan et al. 2015). To facilitate the dimensional analysis, choosing ρ , g , and h_t as repeating variables. Applying the Buckingham π theorem, the non-dimensional form of Equation 1 describing equilibrium downstream scour depth (d_{s_a}) can be derived as Equation 2:

$$\frac{d_{s_a}}{h_t} = \left(\frac{U_0}{U_c}, \frac{z}{h_t}, \frac{d_{50}}{h_t}, \frac{2\alpha}{\pi} \right) \quad (2)$$

Where:

- d_{s_a}/h_t = relative equilibrium downstream scour depth,
- U_0/U_c = flow intensity,
- z/h_t = relative weir height,
- d_{50}/h_t = relative sediment size (sediment coarseness), and
- $2\alpha/\pi$ = normalized upstream face angle

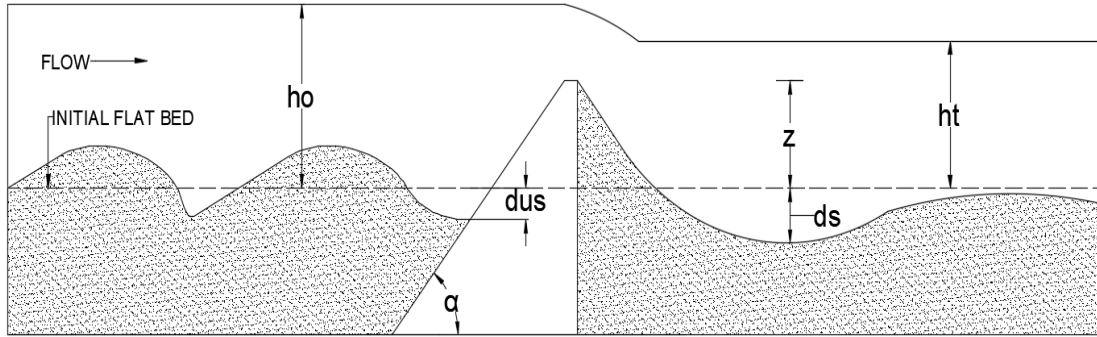


Figure 1 Schematic drawing local scour at submerged weir.

3. DATA FOR ANALYSIS

In the present study, 217 datasets from the literature have been gathered and reanalyzed a comprehensive 217 datasets from the literature, encompassing various significant studies on scour depth at submerged weirs. The data sources include seminal works by Guan et al. (2013), Guan et al. (2015), Guan et al. (2016), as well as more recent contributions by Wang et al. (2018a; 2018b), and Wang et al. (2019). This extensive dataset allows for a detailed analysis and modeling of the complex processes governing scour depth, leveraging the strengths of both traditional and soft computing approaches. The details of the data sets used in the present study are summarized in Table 1.

Table 1 Parameters used for modeling relative equilibrium downstream scour depth.

Parameters	Data range		Data statistics	
	Minimum	Maximum	Mean	COV
d_{s_a}/h_t	0.133	1.506	0.612	0.451
U_o/U_c	0.722	3.748	2.188	0.332
z/h_t	0.000	0.344	0.205	0.304
d_{50}/h_t	0.00173	0.00708	0.004	0.417
$2\alpha/\pi$	0.166	1	0.894	0.264

4. METHODOLOGY

In this study, different scour depth prediction models were developed using a comprehensive dataset collected from existing literature. The evaluation of accuracy and reliability of the developed models was assessed using several standard performance indices such as correlation coefficient (R), mean percentage error (MPE), mean absolute deviation (MAD), and root mean square error (RMSE). These performance indices were used by various researchers (Niazkar and Zakwan 2021; Zakwan 2018) and proved to be best for evaluating the model's prediction capability. The equations of correlation coefficient (R), mean percentage error (MPE), mean absolute deviation (MAD), and root mean square error (RMSE) are given Equation 3, Equation 4, Equation 5, and Equation 6, respectively.

$$\text{Correlation Coefficient (R)} = \frac{N(\sum_{i=1}^N X_i Y_i) - (\sum_{i=1}^N X_i)(\sum_{i=1}^N Y_i)}{\sqrt{[N \sum_{i=1}^N X_i^2 - (\sum_{i=1}^N X_i)^2][N \sum_{i=1}^N Y_i^2 - (\sum_{i=1}^N Y_i)^2]}} \quad (3)$$

$$\text{Mean Percentage Error (MPE)} = \frac{100\%}{N} \left[\sum_{i=1}^N \left(\frac{X_i - Y_i}{X_i} \right) \right] \quad (4)$$

$$\text{Mean Absolute Deviation (MAD)} = \frac{1}{N} \left[\sum_{i=1}^N |Y_i - \bar{Y}_i| \right] \quad (5)$$

$$\text{Root Mean Square Error (RMSE)} = \sqrt{\frac{\sum_{i=1}^N (X_i - Y_i)^2}{N}} \quad (6)$$

Where:

X_i = observed relative equilibrium downstream scour depth,

Y_i = predicted relative equilibrium downstream scour depth,

\bar{Y}_i = mean of predicted relative equilibrium downstream scour depth, and \bar{Y}_i

N = total number of observations.

Non-linear regression models were developed using MATLAB 2016a software (The MathWorks, Inc. 2016). While regression analysis is a traditional approach for modeling relationships in data, it has some notable limitations. As Uyumaz et al. (2006), pointed out, regression analysis assumes that the scatter points have zero deviation from the fitted curve, which is often not true for all data points. The fitting curve may pass closely through several points, but this does

not guarantee accuracy across the entire dataset. Additionally, regression models typically assume that errors follow a Gaussian distribution and are independent of each other, assumptions that do not hold in many practical scenarios. Given these drawbacks, researchers such as Johnson and Ayyub (1996) and Uyumaz et al. (2006) have suggested exploring alternative modeling approaches to overcome the limitations of regression analysis. Artificial Neural Networks (ANN) and Adaptive Neuro-Fuzzy Inference Systems (ANFIS) offer robust alternatives to traditional regression techniques. These models are particularly adept at capturing non-linear and complex relationships in data, which are common in hydraulic engineering problems. In this study, ANN, including Feed Forward Back Propagation (FFBP), Radial Basis Function (RBF), General Regression Neural Network (GRNN), and ANFIS models, were developed to predict the relative downstream scour depth at submerged weirs.

4.2 Artificial Neural Network (ANN)

Artificial Neural Networks (ANN) are a powerful soft computing technique based on how the human brain processes information. ANNs learn and generate knowledge by mimicking the brain's network of neurons, using interconnected nodes arranged in structured layers. Each node is a fundamental processing element analogous to a biological neuron. These nodes include an activation function that transforms the input signals into output signals, effectively capturing the complex, non-linear relationships between predictors and target variables.

ANN Structure and Function

1. **Nodes (Neurons):** These are the computational units within the network. Each node processes input information and applies an activation function to produce an output.
2. **Layers:** ANNs are organized into layers. Input Layer- Receives the input signals. Hidden Layer- Intermediates between input and output, where the actual learning and feature extraction take place. Output Layer- Provides the final prediction or classification output.
3. **Activation Function:** The activation function within each node determines the node's output based on the weighted sum of its inputs. Standard activation functions include sigmoid, tanh, and ReLU (Rectified Linear Unit), which introduce non-linearity into the model, allowing it to learn and model complex patterns in the data.

ANN Learning Algorithms

Different learning algorithms within ANN frameworks enable the network to adjust its weights and biases during training, enhancing its ability to model non-linear systems effectively. This study employs three learning algorithms to model the relative equilibrium scour depth.

1. In FFBP, data flows through the network from the input to the output layer. The network is trained using backpropagation, where the error between predicted and actual outcomes is propagated back through the network to update weights and minimize errors. FFBP is widely used due to its simplicity and effectiveness in learning complex mappings from input to output. The working structure of the FFBP network is shown in Figure 2.

2. Radial Basis Function (RBF): RBF networks use radial basis functions as activation functions. They measure the distance between input vectors and the centre of radial basis functions. The output is a weighted sum of these functions. RBF is particularly effective for problems where data clusters in certain regions, making it suitable for approximating functions and interpolation. The working structure of RBF network is shown in Figure 3.
3. Generalized Regression Neural Network (GRNN): GRNN is a type of probabilistic neural network used for regression problems. It predicts continuous values by averaging the weighted contributions of training samples, where weights are determined by the distance between the input and the training samples. GRNN is known for its fast-learning process and robust performance with noisy data. The working structure of the RBF network is shown in Figure 4.

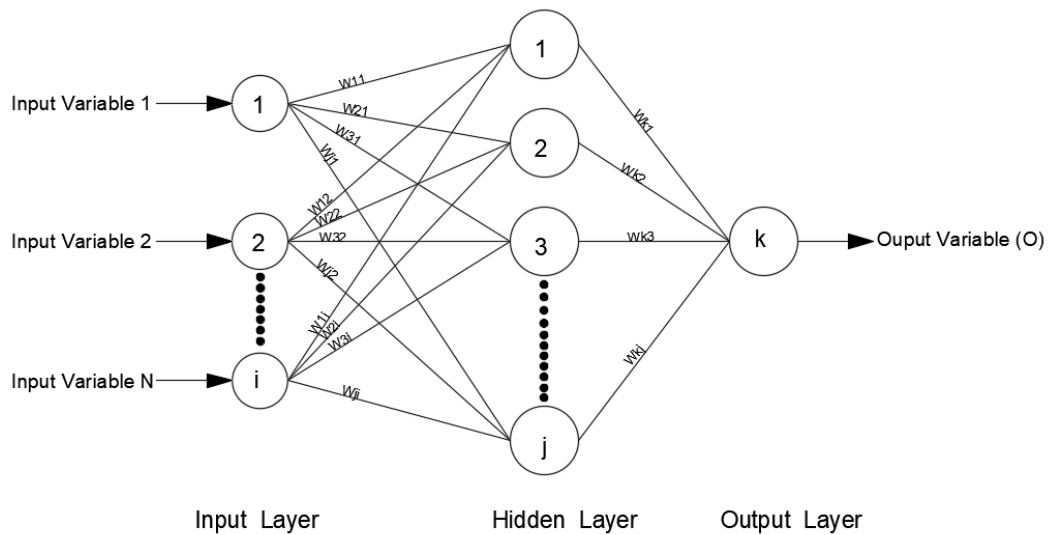


Figure 2 Structure of FFBP neural network.

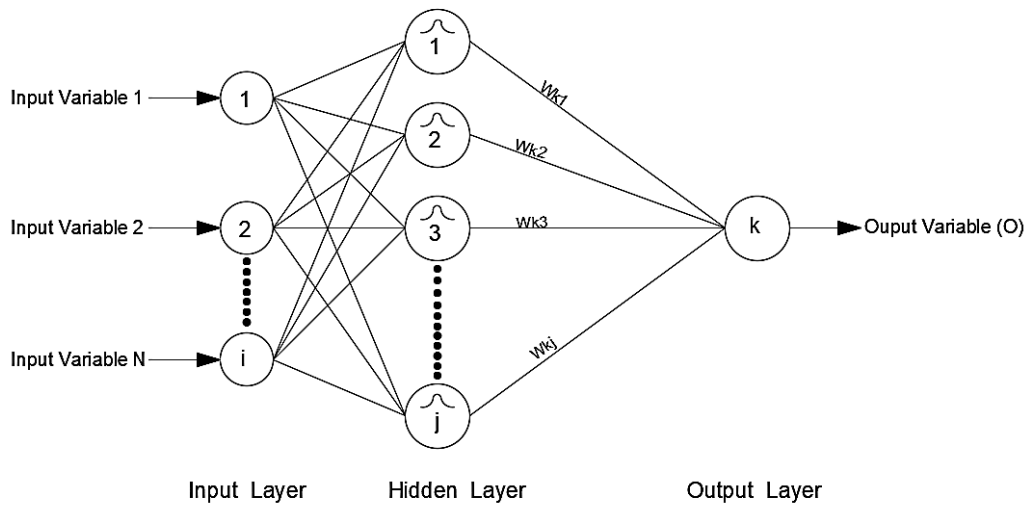


Figure 3 Structure of Radial Basis Function Neural Network.

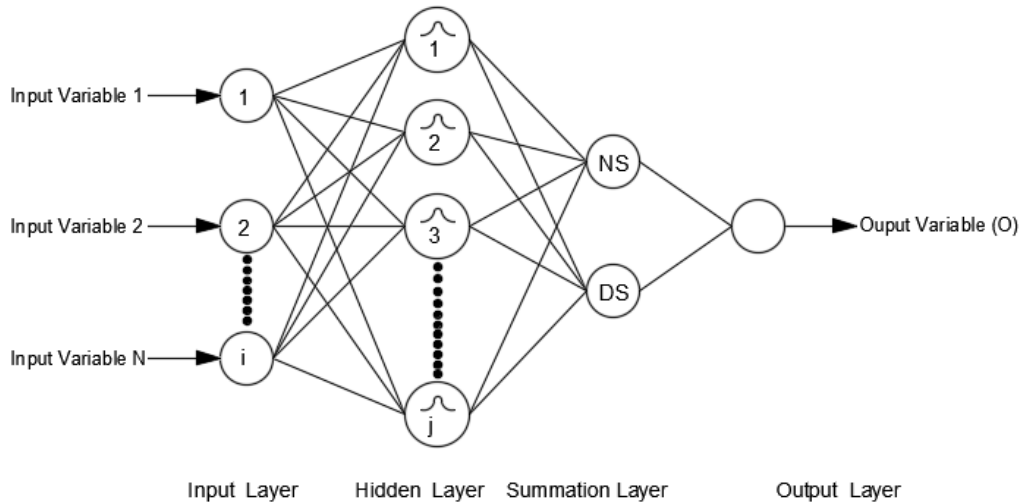


Figure 4 Structure of Generalized Regression Neural Network (GRNN).

4.3 Adaptive Neuro Fuzzy Inference System (ANFIS)

Adaptive Neuro-Fuzzy Inference System (ANFIS) combines the strengths of both Artificial Neural Networks (ANN) and Fuzzy Inference Systems (FIS). ANFIS inherits the ability of ANN to learn from data, adjusting its parameters through training to minimize errors. It also incorporates the FIS's ability to model complex systems through intuitive, human-readable IF-THEN rules and membership functions, which describe how each input variable affects the output. This hybrid approach utilizes neural network principles to construct a set of fuzzy IF-THEN rules and appropriate membership functions, bridging the gap between numerical data-driven learning and linguistic reasoning. In this study, the Takagi-Sugeno (T-S) model of FIS is employed within the ANFIS framework. The T-S model is particularly suited for dealing with non-linear and complex systems due to its ability to handle multi-variable and multi-output systems with precision. Here is a simplified example to illustrate its application. Consider two input variables, M and N , and one output (O). The working structure of the Takagi-Sugeno ANFIS model with two inputs and two rules is shown in Figure 5. The Takagi-Sugeno model uses rules that directly relate inputs to outputs through linear equations or constants in the consequent part. The rules for our example can be formulated as follows:

- Rule 1: If M is X_1 and N is Y_1 , then $O_1 = a_1M + b_1N + c_1$
- Rule 2: If M is X_2 and N is Y_2 , then $O_2 = a_2M + b_2N + c_2$

Where:

$X_1, X_2,$ and Y_1, Y_2 = membership function values of each input M and N , and
 $a_1, b_1, c_1,$ and a_2, b_2, c_2 = linear parameters of the Takagi-Sugeno FIS model.

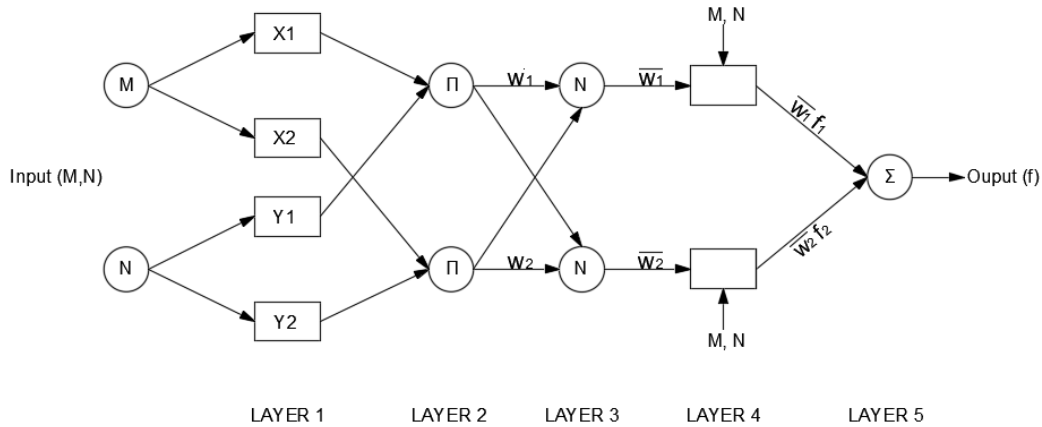


Figure 5 Structure of Takagi-Sugeno ANFIS model with two inputs and two rules.

5 RESULTS AND DISCUSSION

5.1 Performance of existing scour depth prediction models

Scour depth prediction models proposed by Guan et al. (2013), Guan et al. (2015), Guan et al. (2016), Wang et al. (2018a), and Wang et al. (2019) were used in the present for comparative analysis. Initially, the performance of these prediction models was assessed using their respective laboratory data sets, the same data sets that were originally used to develop them in literature. This step ensures that each model is tested within the data range it was designed for, and results are reported in Table 2.

Table 2 Performance of existing regression models based on respective data sets.

Prediction model	Correlation coefficient (R)	Mean Percentage Error (MPE)	Mean Absolute Deviation (MAD)	Root Mean Square Error (RMSE)
Guan et al. (2013)	0.949	0.966	0.389	0.150
Guan et al. (2015)	0.981	0.463	0.238	0.071
Guan et al. (2016)	0.886	-51.361	0.231	0.250
Wang et al. (2018a)	0.893	-43.651	0.250	0.267
Wang et al. (2019)	0.582	11.186	0.187	0.290

5.2 Comparative performance of the existing scour depth prediction models and present study's regression model

A non-linear regression analysis was carried out using MATLAB 2016a software for the conventional regression model. The entire dataset (100% datasets) was utilized to develop this model, ensuring comprehensive representation and accuracy. The resulting regression model is presented below.

$$\frac{d_{s,a}}{h_t} = 0.884 \left(\frac{U_0}{U_c}\right)^{0.686} \left(\frac{z}{h_t}\right)^{1.162} \left(\frac{d_{50}}{h_t}\right)^{-0.173} \left(\frac{2\alpha}{\pi}\right)^{0.136} \quad (7)$$

A comparative analysis was conducted to evaluate the prediction performance of the developed regression model (Equation 7). The relative scour depths were predicted using a regression

model (Equation 7) and previously available scour depth prediction models in the literature. This study utilized the entire collection of data sets (100%) for comparative analysis. This comprehensive evaluation is crucial because it tests the robustness and generalizability of the models when applied to a broader range of conditions beyond their original development data. These results are reported in Table 3. Guan et al. (2015) and Wang et al. (2018a) models demonstrate the best generalizability, maintaining high correlation and low error metrics even when applied to the full data set. This suggests they are more robust and adaptable to various conditions. Models like Guan et al. (2013) and Guan et al. (2016), which performed well on their original data sets, exhibit significant performance degradation when tested on broader data sets, highlighting their limited applicability to new conditions. Guan et al. (2016) and Wang et al. (2018a) models show significant negative biases with MPE values of -51.361% and -43.651%, respectively, on their original data sets. This suggests these models tend to underpredict the scour depth significantly. When evaluated on the full data set, these models still show considerable biases with MPE values of 50.554% and 36.421%, indicating that they are not well-suited to predict outside their training conditions. While biases with positive MPE in Wang et al. (2019) suggest an overestimation of scour depth. The present study regression model (Equation 7) shows strong generalization capabilities, comparable to Guan et al. (2015), with good overall performance metrics. It also provides a balanced approach with controlled biases and errors, indicating a good trade-off between prediction accuracy.

Table 3 Performance of existing and present study's regression model based on full data sets.

Prediction model	Correlation coefficient (R)	Mean Percentage Error (MPE)	Mean Absolute Deviation (MAD)	Root Mean Square Error (RMSE)
Guan et al. (2013)	0.528	6.945	0.539	1.084
Guan et al. (2015)	0.825	-4.360	0.256	0.180
Guan et al. (2016)	0.709	50.554	0.156	0.362
Wang et al. (2018a)	0.870	-36.421	0.270	0.246
Wang et al. (2019)	0.508	21.204	0.200	0.319
Regression model (Equation 7)	0.722	-5.396	0.258	0.193

5.3 Comparative performance of the present study's regression, ANN, and ANFIS models

For regression, ANN, and ANFIS model development, a randomly selected 80% of the data set was used for training, while the remaining 20% was reserved for validation. This approach helps ensure that the model learns the underlying patterns in the data without overfitting. Non-linear regression analysis was performed using MATLAB 2016a software. The resulting regression model is provided below.

$$\frac{d_{s,a}}{h_t} = 1.094 \left(\frac{U_0}{U_c}\right)^{0.677} \left(\frac{z}{h_t}\right)^{1.216} \left(\frac{d_{50}}{h_t}\right)^{-0.155} \left(\frac{2\alpha}{\pi}\right)^{0.152} \quad (8)$$

Similarly, ANN and ANFIS models were developed using MATLAB software. In this study, the relative downstream scour depth at a submerged weir was modelled using three different ANN learning algorithms: Feed Forward Back Propagation (FFBP), Radial Basis Function (RBF), and Generalized Regression Neural Network (GRNN). For the FFBP models, various combinations of

the number of hidden layer nodes and activation functions were tested to determine the optimal configuration. The best-performing FFBP model was found to have 7 hidden layer nodes. This model was trained using the Levenberg-Marquardt algorithm, and the tan-sigmoid activation function was used for both the hidden and output layers. Similarly, for the RBF models, different values of spread radius were explored. The optimal configuration for the RBF model included 32 hidden layer nodes with a spread radius of 1.5. For the GRNN models, the optimal setup involved 6 hidden layer nodes and a spread radius of 0.9. The ANFIS network was developed using the subtractive clustering method, with the Neuro-Fuzzy Design Toolbox in MATLAB software. Multiple ANFIS models were generated by experimenting with different values of the cluster radius. Through a trial-and-error approach, the optimal cluster radius was determined to be 0.5. The performance indices of regression, FFBP, RBF, GRNN and ANFIS models during the training and validation phase are represented in Table 4. The scatter plot of the regression (Equation 8), FFBP, RBF, GRNN, and ANFIS model during the training and validation phase is shown in Figure 6.

The FFBP model during training demonstrated strong performance with an R value of 0.974, indicating a very high degree of the linear relationship between the predicted and observed values. The MPE of -1.224% shows a slight underestimation in the predictions. The MAD and RMSE values were 0.237 and 0.065, respectively, suggesting low deviation and errors in the predictions. During validation, the FFBP model maintained a high R value of 0.952, though slightly lower than in training, showing good generalization ability. The MPE of -6.533% indicates more underestimation compared to training. The MAD was 0.203, and the RMSE increased slightly to 0.081, which is expected as the model adjusts to new data. The RBF model during training achieved an R value of 0.969, which is slightly lower than the FFBP but still indicates a strong linear relationship. The MPE of -1.158% is quite low, showing minimal underestimation. The MAD and RMSE values were 0.219 and 0.068, respectively, demonstrating good accuracy. For validation, the RBF model's R value dropped to 0.876, indicating a decrease in performance when applied to new data. The MPE of -3.408% is still relatively low, and the MAD was 0.213. The RMSE increased to 0.131, suggesting the model struggles slightly more with unseen data compared to FFBP. The GRNN model showed good performance during training with an R value of 0.952. The MPE of -1.948% indicates a small underestimation. MAD and RMSE values were 0.220 and 0.086, respectively, reflecting reasonable accuracy. In validation, the GRNN model's R remained high at 0.950, showing strong consistency in performance. The MPE of -0.986% is very low, indicating minimal bias. The MAD and RMSE were 0.198 and 0.072, respectively, suggesting that GRNN handles new data well and maintains accuracy. The ANFIS model during training had an R value of 0.940, slightly lower than the neural network models but still strong. The MPE of -2.861% indicates some underestimation. The MAD was 0.114, notably low, and the RMSE was 0.174, indicating moderate prediction error. The ANFIS model's R was 0.937 during validation, consistent with its training performance. The MPE of -5.742% suggests moderate underestimation. MAD and RMSE values were 0.165 and 0.242, respectively, indicating reasonable accuracy and generalization to new data. The regression model (Equation 8) achieved an R value of 0.724, significantly lower than the soft computing models, indicating a weaker linear relationship between predicted and observed values. The MPE of -6.266% shows a tendency towards underestimation. The MAD was 0.180, and the RMSE was 0.195, indicating higher deviation and error compared to the other models. In validation, the regression model's R was 0.731, similar to its training phase.

The MPE of -11.956% reflects a considerable underestimation. The MAD was 0.205, and the RMSE remained at 0.195, consistent with the training results but still less accurate than the soft computing techniques. FFBP and GRNN neural networks outperformed the traditional regression model regarding accuracy and generalization. The FFBP model consistently showed the highest correlation and lowest error metrics, making it the study's most reliable predictor of downstream scour depth. ANFIS also performed well, especially in terms of MAD during training, highlighting its effectiveness in dealing with complex, non-linear relationships. The regression model, while useful, demonstrated significantly lower predictive performance compared to the soft computing techniques, suggesting that these advanced models are better suited for capturing the complexities of scour depth prediction at submerged weirs.

Table 4 Performance of ANN, ANFIS models over regression model.

Performance Index		Correlation Coefficient (R)	Mean Percentage Error (MPE)	Mean Absolute Deviation (MAD)	RMSE
FFBP model	Training	0.974	-1.224	0.237	0.065
	Validation	0.952	-6.533	0.203	0.081
RBF model	Training	0.969	-1.158	0.219	0.068
	Validation	0.876	-3.408	0.213	0.131
GRNN model	Training	0.952	-1.948	0.220	0.086
	Validation	0.950	-0.986	0.198	0.072
ANFIS model	Training	0.940	-2.861	0.114	0.174
	Validation	0.937	-5.742	0.165	0.242
Regression model (Equation 8)	Training	0.724	-6.266	0.180	0.195
	Validation	0.731	-11.956	0.205	0.195

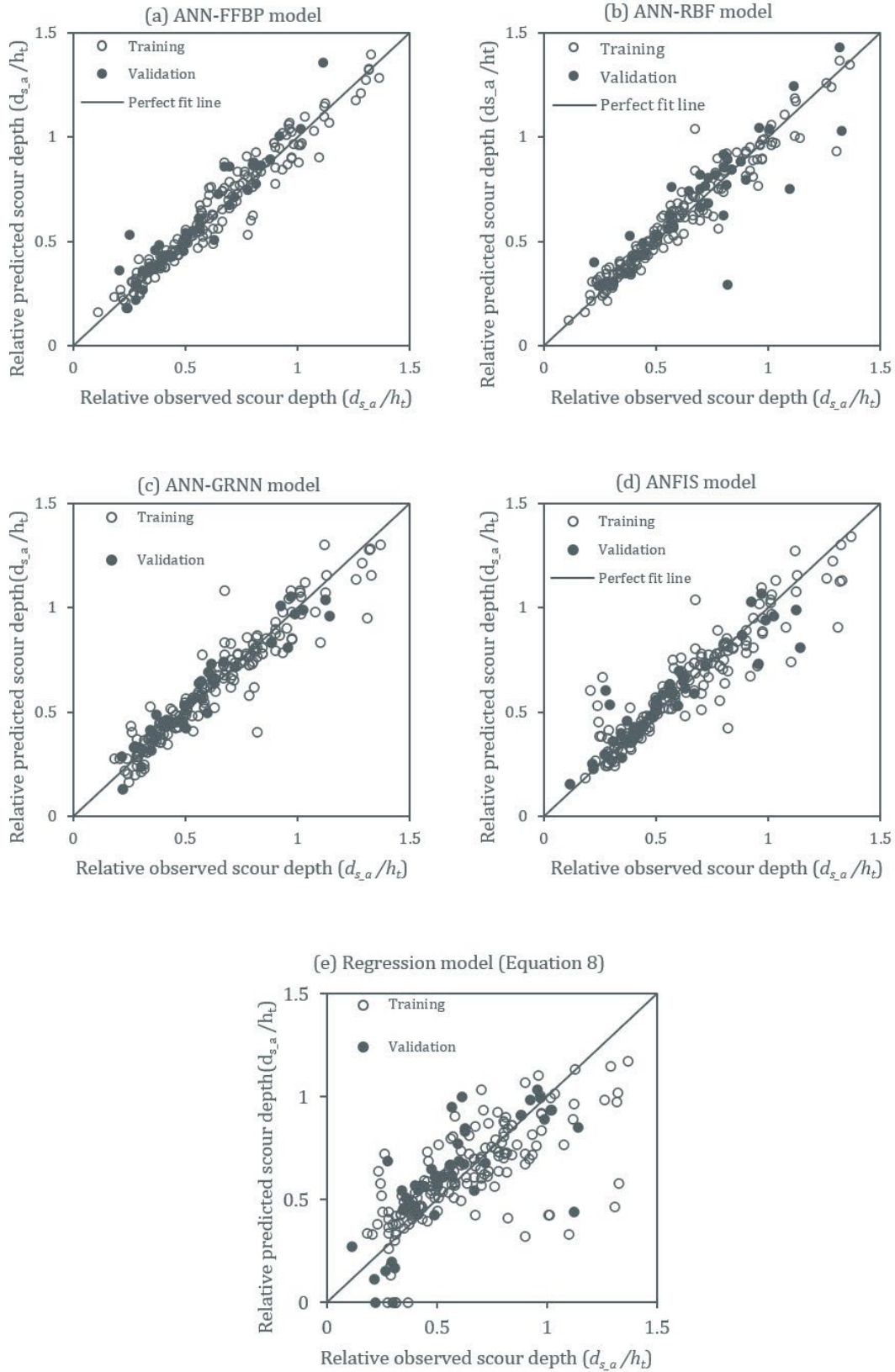


Figure 6 Scatter diagrams of relative observed and predicted scour depth by present study's models.

6. SENSITIVITY ANALYSIS

The sensitivity analysis aimed to determine the influence of various predictor variables on the relative scour depth at a submerged weir. Sensitivity analysis was performed on the FFBP model as it produced the highest correlation and lowest error metrics, making it more effective than RBF, GRNN, ANFIS, and regression. By systematically removing one predictor variable at a time and observing the changes in FFBP model performance, the significance of each variable can be assessed. The results are summarized in Table 5. Model 1, using all four predictor variables, achieves the highest correlation coefficient ($R = 0.964$) and the lowest RMSE (0.071). This suggests that when all these factors are considered together, the model predicts the relative scour depth most accurately. Removing the upstream weir slope ($2\alpha/\pi$) in Model 2, slightly reduces the correlation coefficient to 0.931 and increases the RMSE to 0.096. This indicates that while the slope has an effect, it is not as critical as some other variables, but it still contributes to overall accuracy. Excluding the relative sediment size (d_{50}/h_t) in Model 3, results in a further reduction in the correlation coefficient to 0.915 and an increase in RMSE to 0.104. This suggests that sediment size also plays a significant role but is less dominant than the flow intensity and relative weir height. When the relative weir height (z/h_t) is removed in Model 4, the correlation coefficient drops significantly to 0.736, and the RMSE increases to 0.138. This demonstrates that weir height is crucial in predicting scour depth. Omitting flow intensity (U_0/U_c) in Model 5 results in the lowest correlation coefficient (0.621) and the highest RMSE (0.144). This indicates that flow intensity is the most important factor among the predictor variables. Its exclusion leads to the most significant decline in model performance, underscoring its critical influence on scour depth.

Table 5 Sensitivity analysis for predictor variables.

Model	Target variable	Predictor variable	Correlation Coefficient (R)	Root Mean Square Error (RMSE)
1	$\frac{d_{s,a}}{h_t}$	$\frac{U_0}{U_c}, \frac{z}{h_t}, \frac{d_{50}}{h_t}, \frac{2\alpha}{\pi}$	0.964	0.071
2	$\frac{d_{s,a}}{h_t}$	$\frac{U_0}{U_c}, \frac{z}{h_t}, \frac{d_{50}}{h_t}$	0.931	0.096
3	$\frac{d_{s,a}}{h_t}$	$\frac{U_0}{U_c}, \frac{z}{h_t}, \frac{2\alpha}{\pi}$	0.915	0.104
4	$\frac{d_{s,a}}{h_t}$	$\frac{U_0}{U_c}, \frac{d_{50}}{h_t}, \frac{2\alpha}{\pi}$	0.736	0.138
5	$\frac{d_{s,a}}{h_t}$	$\frac{z}{h_t}, \frac{d_{50}}{h_t}, \frac{2\alpha}{\pi}$	0.621	0.144

7. CONCLUSIONS

The study demonstrates that ANN models (FFBP, RBF, and GRNN) significantly outperform conventional regression models in predicting downstream scour depth at submerged weirs. These models provide greater accuracy and robustness, making them highly suitable for addressing complex hydraulic engineering problems. The ANFIS model also proved effective, especially in its ability to blend neural network learning with fuzzy logic. These findings highlight

the potential of leveraging modern computational approaches to enhance predictive modeling in hydraulic engineering. The sensitivity analysis reveals that the flow intensity (U_o/U_c) and the relative weir height (z/h_t) are the most influential predictors in modeling the relative scour depth at a submerged weir. When these variables were included, the high correlation coefficients and low RMSE values confirmed their significant impact. Conversely, the model's performance substantially degrades when either of these variables is omitted. Relative sediment size (d_{50}/h_t) also affects the relative scour depth but not as much as flow intensity (U_o/U_c) and the relative weir height (z/h_t). The upstream weir slope ($2\alpha/\pi$) has moderate effect on relative scour depth. Hence, for accurate scour depth prediction, it is essential to consider these dominant factors.

Therefore, the present study models (ANN and ANFIS) will help to predict scour depth more precisely. This will result in the safe and economical design of submerged weirs. Furthermore, studies can be carried out in predicting scour depth using other soft computing techniques and uncertainty analysis can also be carried out for input variables.

NOTATIONS

ANN	artificial neural network
d_{50}	median size of particle
d_s	observed downstream scour depth
d_{s_a}	observed equilibrium downstream scour depth
d_{us}	observed upstream scour depth
FFBP	feed-forward back propagation
FFCC	feed forward cascade correlation
GEP	genetic expression programming
GMDH	group method of data handling
h_o	approach flow depth
h_t	tail water depth
R	correlation coefficient
$t \cdot e$	normalized time to reach equilibrium scour depth
U_c	critical average approach flow velocity
U_o	average approach flow velocity
W_{kj}	connection weight between the k^{th} node of the output layer and the j^{th} node of the hidden layer
α	upstream weir face angle
μ	dynamic viscosity
ρ_s	sediment density

REFERENCES

- Azamathullah, H.M., M.C. Deo, and P.B. Deolalikar. 2005. "Neural networks for estimation of scour downstream of a ski-jump bucket." *Journal of Hydraulic Engineering* 151 (10): 898–908. [https://doi.org/10.1061/\(ASCE\)0733-9429\(2005\)131:10\(898\)](https://doi.org/10.1061/(ASCE)0733-9429(2005)131:10(898))
- Azamathullah, H.M., A.A. Ghani, and N.A. Zakaria. 2009. "ANFIS-based approach to predicting scour location of spillway." *Proceedings ICE Water Management* 162, 399–407.
- Bormann, N, and P.Y. Julien. 1991. "Scour downstream of grade-control structures." *Journal of Hydraulic Engineering* 117 (5): 579–594. [https://doi.org/10.1061/\(ASCE\)0733-9429\(1991\)117:5\(579\)](https://doi.org/10.1061/(ASCE)0733-9429(1991)117:5(579))
- Farhoudi, J., S.M. Hosseini, and M. Sedghi-Asl. 2010. "Application of neuro-fuzzy model to estimate the characteristics of local scour downstream of stilling basins." *Journal of Hydroinformatics*. 12 (2): 201–211. <https://doi.org/10.2166/hydro.2009.069>
- Gaudio, R., A. Marion, and V. Bovolin. 2000 "Morphological effects of bed sills in degrading rivers." *Journal of Hydraulic Research* 38 (2): 89–96. <https://doi.org/10.1080/00221680009498344>
- Guan, D., B.W. Melville, and H. Friedrich. 2013. "Bed load influence on scour at submerged weirs." *Proceedings of 2013 IAHR World Congress*, September 8-13, 2013, pp. 9.
- Guan, D., B.W. Melville, and H. Friedrich. 2014a. "Flow patterns and turbulence structures in a scour hole downstream of a submerged weir." *Journal Hydraulic Engineering* 140 (1), 68–76. [https://doi.org/10.1061/\(ASCE\)HY.1943-7900.0000803](https://doi.org/10.1061/(ASCE)HY.1943-7900.0000803)
- Guan, D., B.W. Melville, and H. Friedrich. 2014b. "A preliminary study on scour at submerged weir in live bed conditions." In *River Flow 2014*, CRC Press.
- Guan, D., B.W. Melville, and H. Friedrich. 2015. "Live-bed scour at submerged weirs." *Journal of Hydraulic Engineering* 141 (2): 0401407, 1–12. [https://doi.org/10.1061/\(ASCE\)HY.1943-7900.0000954](https://doi.org/10.1061/(ASCE)HY.1943-7900.0000954)
- Guan, D., B.W. Melville, and H. Friedrich. 2016. "Local scour at submerged weirs in sand-bed channels." *Journal of Hydraulic Research* 54 (2): 172–184. <https://doi.org/10.1080/00221686.2015.1132275>
- Guan, D., L. Wang, L. Ma, and B.W. Melville. 2022. "Fluctuating Frequency of Live Bed Scour Depth around Submerged Weirs at Equilibrium Stages." *Journal of Hydraulic Engineering* 148 (4): 06022001. [https://doi.org/10.1061/\(ASCE\)HY.1943-7900.0001972](https://doi.org/10.1061/(ASCE)HY.1943-7900.0001972)
- Johnson, P.A., and B.M. Ayyub. 1996. "Modeling Uncertainty in Prediction of Pier Scour." *Journal of Hydraulic Engineering* 122, 2. [https://doi.org/10.1061/\(ASCE\)0733-9429\(1997\)123:9\(822\)](https://doi.org/10.1061/(ASCE)0733-9429(1997)123:9(822))
- Keshavarzi, A., R. Gazni, and S.R. Homayoon. 2012. "Prediction of scouring around an arch-shaped bed sill using neuro-fuzzy model." *Applied Soft Computing Journal* 12, 486–493. <https://doi.org/10.1016/j.asoc.2011.08.019>
- Lenzi, M.A., A. Marion, and F. Comiti. 2003. "Local scouring at grade-control structures in alluvial mountain rivers." *Water Resources Research* 39, 7. <https://doi.org/10.1029/2002WR001815>
- Muzzammil, M., and J. Alam. 2016. "Scour prediction at the control structures using Adaptive Neuro-Fuzzy Interference System." *IWRA (INDIA)* 5 (2): 22–30.

- Niazkar, M., and M. Zakwan. 2021. "Assessment of artificial intelligence models for developing single-value and loop rating curves." *Complexity* 21. <https://doi.org/10.1155/2021/6627011>
- Noori, R., and F. Hooshyaripor. 2014. "Effective prediction of scour downstream of ski-jump buckets using artificial neural networks." *Water Resources* 41, 8–18. <https://doi.org/10.1134/S0097807814010096>
- Roushangar, K., S. Akhgar, A. Erfan, and J. Shiri. 2016. "Modeling scour depth downstream of grade-control structures using data driven and empirical approaches." *Journal of Hydroinformatics* 18 (6): 946–960. <https://doi.org/10.2166/hydro.2016.242>
- Soliman, M. 2007. "Artificial neural network prediction of maximum scour hole downstream of hydraulic structure." *Eleventh International Water Technology Conference, IWTC11 2007 Sharm El-Sheikh, Egypt*.
- The MathWorks, Inc. 2016. *MATLAB Release R2016a*. Natick, Massachusetts, U.S.A.
- Uyumaz, A., A. Altunkaynak, and M. Ozger. 2006. "Fuzzy logic model for equilibrium scour downstream of a dam's vertical gates." *Journal of Hydraulic Engineering* 132, 10. [https://doi.org/10.1061/\(ASCE\)0733-9429\(2006\)132:10\(1069\)](https://doi.org/10.1061/(ASCE)0733-9429(2006)132:10(1069))
- Wang, L., B.W. Melville, and D. Guan. 2018a. "Effects of upstream weir slope on local scour at submerged weirs." *Journal of Hydraulic Engineering* 144 (3): 04018002, 1–9. [https://doi.org/10.1061/\(ASCE\)HY.1943-7900.0001431](https://doi.org/10.1061/(ASCE)HY.1943-7900.0001431)
- Wang, L., B.W. Melville, D. Guan, and C.N. Whittaker. 2018b "Local scour at downstream sloped submerged weirs." *Journal of Hydraulic Engineering* 144 (8): 04018044, 1–8. [https://doi.org/10.1061/\(ASCE\)HY.1943-7900.0001492](https://doi.org/10.1061/(ASCE)HY.1943-7900.0001492)
- Wang, L., B.W. Melville, and D. Guan. 2019. "Scour estimation at downstream of a submerged weir." *Journal of Hydraulic Engineering* 145 (12): 06019016, 1–7. [http://dx.doi.org/10.1061/\(ASCE\)HY.1943-7900.0001654](http://dx.doi.org/10.1061/(ASCE)HY.1943-7900.0001654)
- Wang, L., B.W. Melville, C.N. Whittaker, and D. Guan. 2020. "Temporal evolution of clear-water scour depth at submerged weirs." *Journal of Hydraulic Engineering* 146 (3): 06020001. [https://doi.org/10.1061/\(ASCE\)HY.1943-7900.0001712](https://doi.org/10.1061/(ASCE)HY.1943-7900.0001712)
- Wen, Z., L. Wang, B.W. Melville, D. Guan, C.N. Whittaker, and Y.S. Asaad. 2021. "Characteristics of the flow field within a developing scour hole at a submerged weir." *Journal of Hydraulic Research* 60 (2): 283–294. <https://doi.org/10.1080/00221686.2021.1944928>
- Zakwan, M. 2018. "Spreadsheet-based modelling of hysteresis-affected curves." *Applied Water Science* 8, 101. <https://doi.org/10.1007/s13201-018-0745-3>